Thermodynamic description of the Aluminum-Lithium phase diagram

H. Azza*, N. Selhaoui, S. Kardellass, A. Iddaoudi, L. Bouirden

Laboratory of Thermodynamics and Energy (L.T.E), Faculty of science, University IbnZohr, Agadir, Morocco

*Corresponding Author. E-mail: hassan.smp@gmail.com   ; Tel: (+212694333937)

Abstract

The thermodynamic optimization of the AL-Li binary system was carried out with the help of CALculation of PHAse Diagram (CALPHAD) method. Al_2Li_3, Al_4Li_5 and $AlLi_2$ have been treated as stoichiometric compounds while a solution model has been used for the description of the liquid, FCC_A1 (Al) and BCC_A2 (Li) phases. The non-stoichiometric AlLi phase with a narrow homogeneity range was modeled using a two-sublattice model with a mutual substitution of Al and Li on both Sublattice. The optimization is carried out in the Thermo-calc package. A set of self-consistent thermodynamic parameters are obtained. The calculated phase diagram and thermodynamic properties agree well with the available experimental data.

Keywords: Al-Li system, Thermodynamic description, CALPHAD method, Redlich–Kister equation.

Introduction

The aluminum–lithium alloys are interesting because of their use as a construction material in aerospace, military and automobile industry, as the material for electrodes in high temperature batteries and also as one of the materials for safe storage of hydrogen, an ecological source of energy [1]. Moreover the corrosion studies of aluminum and aluminum alloys are closely related to their wide applications in industry [2].

In order to define the processing conditions for making these alloys and subsequent treatments to obtain the optimum engineering properties, a knowledge of the phase diagram and thermodynamic properties of these alloys is essential.

This present work deals with a reassessment of the thermodynamic description of the Al-Li system using the Calphad method [3]. In this method, the thermodynamic models for the Gibbs energy of all the individual phases are studied using the Parrot module in the Thermo-Calc package [4]. The thermodynamic parameters involved in the models are optimized from the experimental thermodynamic and phase diagram data.

2. Experimental information

2.1. Phase diagram

The Al-Li phase diagram has been investigated by several authors. The results were taken by Okamoto [5]. The crystal structures of various phases and a list of the phases are reported in Table 1. FCC-A1 (α) dissolves up to about 15 at.% Li, thereby decreasing density and increasing Young's modulus. Al-Li based alloys can also be precipitation hardened by metastable coherent α' (Al_3Li) precipitates with the $L1_2$ structure. In spite of the difficulties in handling Li, Al-Li based alloys have found some use as high strength, low density materials [9-11]. They are then typically alloyed with Mg and/or Cu. Two-phase mixtures of FCC-A1 and AlLi (B32 structure) deliver a stable emf of about 300 mV relative to liquid Li, and played some role in the early development of Li batteries [12, 13].

Table 1: Symbols and crystal structures of the stable solid phases in the Al-Li system.

Phase	Composition at.% Li	Pearson symbol	Strukturbericht Designation	Prototype	Ref	Lattice parameters, Å			Ref
						a	b	c	
α (Al)	0 to 15.5	cF4	A1	Cu	[5]				
α'(Al_3Li)*		cP4	$L1_2$	$AuCu_3$	[5]				
β (AlLi)	46 to 57	cF16	B32	NaTl	[5]	6.36	-	-	[7]
Al_2Li_3	60	hR15	…	Ga_2Te_3	[5]	4.508		14.259	[7]
$AlLi_2$	64 to 66.5	oC12	…	$GaLi_2$	[6]	4.657	9.767	4.490	[8]
Al_4Li_9	69.2	mC26	…	Al_4Li_9	[5]	18.916 19.151	4.5041 5.429	5.4249 4.499	[8] [7]
(Li)	100	cl2	A2	²W	[5]				

*Metastable phase

  The Al-Li system contains three stable intermediate phases; β (AlLi), Al_2Li_3 and Al_4Li_9, There is also a metastable intermediate phase α'(Al_3Li). The phase diagram is dominated by the AlLi phase, which shows a considerable homogeneity range and melts congruently a round 975 K. The phases Al_2Li_3 and Al_4Li_9 show narrow, but essentially unknown, homogeneity ranges. They are treated as stoichiometric in this work.

  The Investigation of the Li rich part of the binary Al–Li system revealed the existence of a new phase, orthorhombic $AlLi_2$ ($AlLi_2$ possesses most likely a small homogeneity range $Al_{1+x}Li_{2-x}$). The crystal structure was determined from single crystal X-ray diffraction data. Refinement of atomic position site occupancies yielded composition $Al_{1.08}Li_{1.92}$ (64 at.% Li) indicating a small homogeneity range, $Al_{1+x}Li_{2-x}$ is the peritectic decomposition product of the stoichiometric compound Al_4Li_9, which is stable below 543 ± 2 K. $AlLi_2$ itself decomposes peritectically to Al_2Li_3 and Li rich melt at 608 ± 2 K. The discovery of $AlLi_2$ ($Al_{1+x}Li_{2-x}$) settles a long standing inconsistency in the Al–Li phase diagram which was based on the assumption that Al_4Li_9 possesses a high temperature modification [8]. Solid lithium dissolves small, but unknown, amount of aluminum [4].

  The crystal structure of Al_2Li_3 was determined by Tebbe et al. [14] and the crystal structure of Al_4Li_9 was determined by Hansen and Smith [15]. The most extensive and consistent investigation of the phase diagram has been made by Schürmann and Voss [16]. Unfortunately, they misinterpreted their results for high Li contents and assigned a high Al solubility in bcc-Li and did not identify the Al_4Li_9 phase. They also assigned the composition $AlLi_2$ to the Al_2Li_3 phase. When assigned to the correct equilibria, their liquidus data and invariant temperatures appear to be reasonable, though. There is a very good agreement among the sources on the invariant temperatures and a good agreement on the liquidus on the Al rich side of the system, but a very large scatter on the liquidus on the Li-rich side. Recent data on the Li-rich liquidus from Pulham et al. [17] are in good agreement with the data from Schürmann and Voss [16]. The difference between the melting temperature of pure Li and the eutectic temperature is insignificant, suggesting that the Al solubility in bcc-Li is small. There is no direct measurement.

  The β (AlLi) phase is stable approximately in the range $0,45 < x_{Li} < 0,56$. There is a large scatter among the experimental data [16, 18–23], both regarding the absolute values and their temperature dependence. The most reasonable and internally consistent data are those of Wen et al. [21] and those of Amezawa et al. [23], both using emf methods. The difference between the two sources is quite large, though, and no preference could be given to one or the other.

2.2. Thermodynanic data

  The enthalpy of formation is measured by several authors, such as Hallstedt et al. [6], Saunders et al. [24] and Sluiter et al. [25]. The enthalpy of formation at 959 ± 4 K of the AlLi, Al_2Li_3 and Al_4Li_9 intermetallic phases was measured by Gasior et al. [26] with the use of the two calorimetric techniques. The first phase was examined by the solution and the direct reaction calorimetric method, and the other two phases only by the solution method. The value of the formation enthalpy measured for the AlLi phase in the case of the solution and direct synthesis technique was equal to -20.7 ± 0.5 and -20.4 ± 0.2 kJ/mol at., respectively. The same thermodynamic function by the solution method for the Al_2Li_3 and Al_4Li_9 phases was equal to -19.1 ± 0.4 and -15.1 ± 0.2 kJ/mol at, respectively.

J. Mater. Environ. Sci. 6 (12) (2015) 3501-3510
ISSN : 2028-2508
CODEN: JMESCN

Azza et al.

The enthalpy of mixing of the liquid has been measured by Bushmanov and Yatsenko [28] and Moser et al. [29] in good mutual agreement. The partial enthalpy has been measured by Lee and Sommer [30]. Li activities in the liquid have been measured by Hicter et al. [31] and Yatsenko and Saltykova [32], also in good mutual agreement.

3. Assessment procedure

Most of the experimental information mentioned above is selected. Indeed, as experimental phase diagram, we used the review work by Okamoto [5] and Hallstedt et al. [6] which is the experimental phase diagram determined by most authors [33-36]. The thermodynamic optimization of the model parameters of the Gibbs energy expressions is an application of the CALPHAD technique with the help of the PARROT module of the Thermo-Calc software developed by Sundman et al. [4] and Jansson [37]. The program works by minimizing an error sum where each of the selected values is given a certain weight. The weight is chosen by personal judgement and changed by trial and error during the work until most of the selected experimental information is reproduced within the expected uncertainty limits. In order to avoid the formation of an unwanted inverted miscibility gap in the liquid phase of the Al–Li system, thermodynamic constraints were imposed during the optimization with the Redlich–Kister formalism [38], a positive curvature of the liquidus by optimizing $d^2G/dx^2 > 0$ in the atomic composition range $0 < x_{Li} < 1$ and every 50 degrees from the liquidus temperature up to 6000 K, was therefore optimized, enthalpy and entropy of same sign. Start values for the parameters were taken from the work of Saunders [39], except for the β (AlLi) phase. The optimization was carried out in two steps. In the first treatment, β (AlLi) was assumed to be a stoichiometric compound. And in the second, it was treated using a two-sublattice model [4, 40]. The parameters obtained from the first treatment were used as starting values for the second.

4. Thermodynamic models

The modeling done by Hallstedt et al. [6] is believed that the Al-Li system contains three stable intermediate phases AlLi, AL_2Li_3 and AL_4Li_9 but Puhakainen et al. [8] has decouvet a new phase $AlLi_2$ as peritectic decomposition Al_4li_9 of high temperature (542 K) therefore this work takes conseddiration by the new phase.

4.1. Pure elements

The Gibbs energy of the pure element i (i= Al, Li) in the phase ϕ (ϕ =Liquid, FCC_A1and BCC_A2), referred to the enthalpy of its stable state at 298.15 K, is described as a function of temperature by:

$$G_i^{\phi}(T) = {}^0 G_i^{\phi} - H_i^{SER}(298.15K) = a + bT + cT\ln T + dT^2 + eT^3 + fT^7 + gT^{-1} + hT^{-9} \qquad (1)$$

where $H_i^{SER}(298.15K)$ is the molar enthalpy of the element i at 298.15 K in its standard element reference (SER) state, FCC_A1 for Al and BCC_A2 for Li.

In this article, The Gibbs energy functions are taken from the SGTE compilation of Dinsdale [41].

3.1. Solution phases

The solution phase (liquid, FCC_A1 (Al) and BCC_A2 (Li)) were modelled as substitutional solution. The Gibbs energy of one mol of formula unit of phase φ is expressed as the sum of the reference part ${}^{ref}G_i^{\phi}$, the ideal part ${}^{id}G_i^{\phi}$, and the excess part ${}^{exc}G_i^{\phi}$:

$$G_m^{\phi} = {}^{ref} G^{\phi} + {}^{id} G^{\phi} + {}^{exc} G^{\phi} \qquad (2)$$

As used in the Thermo-Calc package [4]:

$$^{ref} G^{\phi}(T) = ({}^0 G_{Al}^{\phi}(T) - H_{Al}^{SER}(298.15K))x_{Al} + ({}^0 G_{Li}^{\phi}(T) - H_{Li}^{SER}(298.15K))x_{Li} \qquad (3)$$

$$^{id} G^{\phi} = RT(x_{Al}lnx_{Al} + x_{Li}lnx_{Li}) \qquad (4)$$

J. Mater. Environ. Sci. 6 (12) (2015) 3501-3510
ISSN : 2028-2508
CODEN: JMESCN

Azza et al.

where R is the gas constant, T the temperature, in Kelvin, x_{Al} and x_{Li} are the fraction of elements Al and Li, respectively.

The excess terms of all the solution phases were modelled by the Redlich-Kister [37] formula:

$$^{exc}G_m^\phi(T) = x_{Li}x_{Al}\left[{}^0L_{Li,Al}^\phi(T) + {}^1L_{Li,Al}^\phi(T)(x_{Li}-x_{Al}) + {}^2L_{Li,Al}^\phi(T)(x_{Li}-x_{Al})^2 + \dots\right] \tag{5}$$

$$^iL_{Li,Al}^\phi(T) = a_i + b_iT \tag{6}$$

where $^iL_{Li,Al}^\varphi(T)$ is the interaction parameter between the elements Li and Al, which is evaluated in the present work the coefficients a_i and b_i are optimized using the PARROT module [4].

3.2. Stoichiometric compounds

The phases Al_2Li_3 and Al_4Li_9 show narrow, but essentially unknown, homogeneity ranges. They are treated as stoichiometric in this work. Of course, in view of what Puhakainen et al. [8]. Wrote, it is hardly justifiable to handle $AlLi_2$ as a stoichiometric phase, but a current lack of experimental information may preclude one from utilizing a two-sublattice model to describe its Gibbs energy.

The Gibbs energy of the stoichiometric compounds $^0G_{A_pB_q}$ is expressed as follows:

$$^0G_{A_pB_q} = p\,{}^0G_A + q\,{}^0G_B + a + bT \tag{7}$$

where ^0G_A and ^0G_B are the Gibbs energy of the pure elements Al and Li respectively, a and b are parameters to be determined.

3.3. Intermediate Phase with Homogeneity Range

In the Al–Li system optimized by Hallstedt and Kim [6], a four sublattice model was applied to describe the compound AlLi in order to cope with the order–disorder transition between BCC (disordered, A2) and AlLi (ordered, B32). In the present work, a two-sublattice model $(AL\%,Li)_{0,5}(Al,Li\%)_{0,5}$ is adopted . The symbol % denotes the major component in the second Sublattice. The reason for adopting the two-sublattice model instead of the four-sublattice model is to simplify the compound AlLi in high-order system [42]. The Gibbs energy function per mole of the formula unit $(Al\%,Li)_{0,5}(Al,Li\%)_{0,5}$ is the following:.

$$G^{(Al\%,Li)_{0,5}(Al,Li\%)_{0,5}} - H_{(Al\%,Li)_{0,5}(Al,Li\%)_{0,5}}^{SER} = y_{Al}^1 y_{Al}^2\,{}^0G^{Al_{0.5}Al_{0.5}} + y_{Al}^1 y_{Li}^2\,{}^0G^{Al_{0.5}Li_{0.5}} + y_{Li}^1 y_{Al}^2\,{}^0G^{Li_{0.5}Al_{0.5}} + y_{Li}^1 y_{Li}^2\,{}^0G^{Li_{0.5}Li_{0.5}}$$

$$+RT\left[m\left(y_{Al}^1 \ln y_{Al}^1 + y_{Li}^1 \ln y_{Li}^1\right) + n\left(y_{Al}^2 \ln y_{Al}^2 + y_{Li}^2 \ln y_{Li}^2\right)\right] + {}^{xs}G_{(Al\%,Li)_{0,5}(Al,Li\%)_{0,5}}^{Al_{0.5}Li_{0.5}} \tag{8}$$

where y_{Al}^1 and y_{Li}^1 denote the site fractions of Al and Li in the first Sublattice, y_{Al}^2 and y_{Li}^2 the site fractions of Al and Ni in the second Sublattice, $^0G^{Al_{0.5}Al_{0.5}}, {}^0G^{Li_{0.5}Al_{0.5}}$ and $^0G^{Li_{0.5}Li_{0.5}}$ are the Gibbs energies of the hypothetical compounds $Al_{0.5}Al_{0.5}, Li_{0.5}Al_{0.5}$ and $Li_{0.5}Li_{0.5}$ respectively. $^0G^{Al_{0.5}Li_{0.5}}$ is the Gibbs energy of the stoichiometric compound $Al_{0.5}Li_{0.5}$.

$$H_{(Al\%,Li)_{0,5}(Al,Li\%)_{0,5}}^{SER} = \left(0.5y_{Al}^1 + 0.5y_{Al}^2\right)H_{Al}^{SER} + \left(0.5y_{Li}^1 + 0.5y_{Li}^2\right)H_{Li}^{SER} \tag{9}$$

$^{xs}G_{(Al\%,Li)_{0,5}(Al,Li\%)_{0,5}}^{Al_{0.5}Li_{0.5}}$ is the excess Gibbs energy expressed by the following expression:

$$^{xs}G_{(Al\%,Li)_{0,5}(Al,Li\%)_{0,5}}^{Al_{0.5}Li_{0.5}} = y_{Al}^1 y_{Li}^1\left(y_{Al}^2 L_{Al,Li:Li}^{Al_{0.5}Li_{0.5}} + y_{Li}^2 L_{Al,Li:Li}^{Al_{0.5}Li_{0.5}}\right) + y_{Al}^2 y_{Li}^2\left(y_{Al}^1 L_{Al:Al,Li}^{Al_{0.5}Li_{0.5}} + y_{Li}^1 L_{Li:Al,Li}^{Al_{0.5}Li_{0.5}}\right) \tag{10}$$

where $L_{Al,Li:e}^{Al_{0.5}Li_{0.5}}$ and $L_{e:Al,Li}^{Al_{0.5}Li_{0.5}}$ represent the interaction parameters between the elements Al and Li in the related Sublattice while the other Sublattice is occupied only by the element e (e = Al and Li). These excess parameters are temperature dependent as:

$$a+bT \tag{11}$$

For both intermetallic compounds, the Wagner-Schottky law [43] was applied as follows:

$$^0G^{Li_{0.5}Al_{0.5}} + {}^0G^{Al_{0.5}Li_{0.5}} = {}^0G^{Li_{0.5}Li_{0.5}} + {}^0G^{Al_{0.5}Al_{0.5}} \tag{12}$$

In order that the hypothetical compounds $Li_{0.5}Li_{0.5}$ and $Al_{0.5}Al_{0.5}$ do not appear in the calculated phase diagram, the values +25000 and +75000 J/mol of atoms, determined by trial and error, were added respectively to GHSERAl and GHSERLi for the AlLi compound, were used and all the thermodynamic parameters were optimized and listed in Table 2.

$$^0G^{Li_{0.5}Li_{0.5}} = GHSERLi + 25000 \tag{13}$$

$$^0G^{Al_{0.5}Al_{0.5}} = GHSERAl + 75000 \tag{14}$$

Table 2: Optimized parameters describing the thermodynamic properties of the AL-Li system

Phase	Thermodynamic models	Parameters (J/mol at)
Liquid	(Al, Li)$_1$	$^0L^{liq} = -43500 + 18*T$ $^1L^{liq} = 13700 - 2.11*T$ $^2L^{liq} = 11175$
FCC_A1	(Al, Li)$_1$(Va)$_1$	$^1L^{FCC\_A1} = -55000 + 12*T$ $^2L^{FCC\_A1} = -4*T$
BCC_A2	(Al, Li)$_1$(Va)$_3$	No excess term
AlLi	(Al)$_{0.5}$:(Li)$_{0.5}$	$G^{AlLi}_{Al:Li} - H^{298.15}_{Al} = 75000 + GHSERAl$ $G^{AlLi}_{Al:Li} - H^{298.15}_{Li} = 25000 + GHSERLi$ $G^{AlLi}_{Al:Li} - 0.5*H^{298.15}_{Al} - 0.5*H^{298.15}_{Li}$ $\quad = 0.5*GHSERAl - 0.5*GHSERLi - 8500 + 5.22*T$ $G^{AlLi}_{Al:Li} - 0.5*H^{298.15}_{Al} - 0.5*H^{298.15}_{Li}$ $\quad = 0.5*GHSERAl - 0.5*GHSERLi + 75000 + 8500 - 5.22*T$ $G^{AlLi}_{Al:Li,Al} = -21399 + 7.35*T$
Al$_2$Li$_3$	(Al)$_{0.4}$:(Li)$_{0.6}$	$G^{Al_2Li_3}_{Al:Li} - 0.4*H^{298.15}_{Al} - 0.6*H^{298.15}_{Li}$ $\quad = 0.4*GHSERAl - 0.6*GHSERLi - 18500 - 0.46*T$
AlLi$_2$	(Al)$_{0.34}$:(Li)$_{0.66}$	$G^{AlLi_2}_{Al:Li} - 0.34*H^{298.15}_{Al} - 0.66*H^{298.15}_{Li}$ $\quad = 0.34*GHSERAl - 0.66*GHSERLi - 15150 + 5.4*T$
Al$_4$Li$_9$	(Al)$_{0.31}$:(Li)$_{0.69}$	$G^{Al_4Li_9}_{Al:Li} - 0.31*H^{298.15}_{Al} - 0.69*H^{298.15}_{Li}$ $\quad = 0.31*GHSERAl - 0.69*GHSERLi - 14530 + 1.22*T$

5. Results and discussions

5.1. The assessed phase diagram

The compositions of the phases and the temperatures involved in the invariant reactions mainly based on the phase diagram of the Al-Li system evaluated by Okamoto [5]. Figure 1 shows the calculated equilibrium phase diagram with the numerous experimental data used in the optimization.
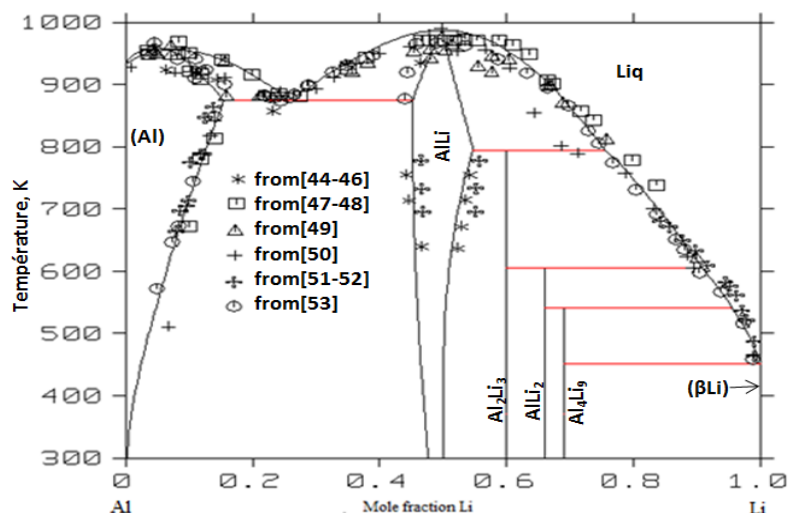
J. Mater. Environ. Sci. 6 (12) (2015) 3501-3510
ISSN : 2028-2508
CODEN: JMESCN

Azza et al.

Figure 1: The calculated Al-Li phase diagram compared with available experimental data [44-53].

A satisfactory agreement is noted. The limit between the (AlLi + (Al)) two-phase domain and the (AL) terminal solid solution is in very satisfactory agreement with the data in [47-48, 50-53]. The liquidus data are described very well. At higher Li content the calculation agrees fairly well with the experimental data of Müller et al. [44] and Pulham et al. [51]. The α (Al) + Liquid two-phase region is very narrow for low Li contents. This was not possible to change without losing the good fit of the liquidus data. For the β (AlLi) phase, composition data are inconclusive (45.2 to 55.9 at. % Li). Thé calculation of thé liquidus is very close to the experimental data of Kishio et al [47], Shamray et al. [49] and Schürmann et al. [53]. The liquidus on the Li rich side calculated in the present work is in best agreement with the experimental data mesured by Williams et al. [48], Voss [52] and Schürmann et al. [53].

The Li-rich region of the Al-Li phase diagram and detail of the Al-rich Al–Li eutectic is plotted in Figure 2. The limit between the (Al_4Li_9 + (βLi)) two-phase domain and the (βLi) terminal solid solution is in very satisfactory agreement with the data in [51-53].The temperature of this Liq ↔ Al_4Li_9 + (βLi) eutectic reaction is calculated at 451.2 K and is therefore in very good agreement with the data of Hallstedt [6] at 452 K, as well as the Li compositions of the liquid eutectic and the (βLi) terminal solid solution.
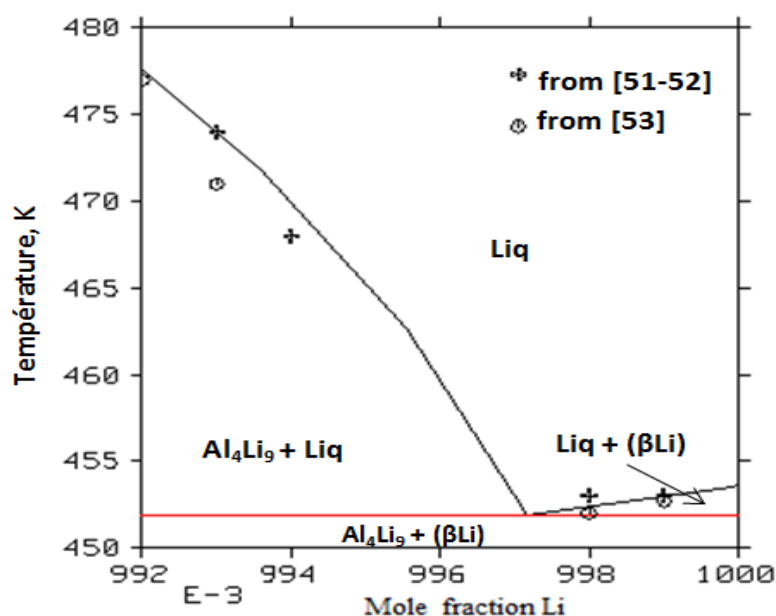

Figure 2: Enlargement of the Li-riche Al-Li euticic region, including experimental data [51-53].

The invariant reactions in the Al-Li system are listed in Table 3 and compared with the results from [6-7]. They are in satisfactory agreement, except the calculated congruent melting of AlLi (T=978.4 K), close to the calculated one (T=975 K) in Kishio et al. [47] but somewhat lower than the experimental one (T = 967 K) in Shamray et al. [49].

Table 3: Invariant reactions in the AL-Li system

Reaction	Reaction type	Values experimental		Reference	This work	
		T/K	x(Li) at		T/K	x(Li) at
Liq ↔ AlLi + Al	Eutectic	875	0.240	[6]	866	0.249
Liq ↔ Al$_4$Li$_9$ + Li	Eutectic	452	0.996	[6]	451.1	0.998
Liq ↔ AlLi	Congruent	975	0.46-0.57	[6]	980	0.45-0.55
Liq + AlLi ↔ Al$_2$Li$_3$	Peritectic	793	0.745	[6]	798	0.785
Liq + Al$_2$Li$_3$ ↔ AlLi$_2$	Peritectic	607 ± 2	0.919	[8]	611	0.937
Liq + AlLi$_2$ ↔ Al$_4$Li$_9$	Peritectic	543 ± 2	0.970	[8]	546	0.971

5.2. Thermodynamics properties

As mentioned previously, the enthalpies of formation of intermetallic compounds are measured by several authors. In general, calorimetric direct measurements are considered to be the most reliable, so the values obtained by Gasior et al. [26] were used in the present study with high weights. The assessed enthalpies of formation of Al-Li intermetallic compounds compared with experimental measurements are plotted in Table 4, also presented in Figure 3.

Table 4: Calculated and measured enthalpies of formation of the intermetallic compounds

Phase	$\Delta_f H$(kj/mol)	Method	reference	This work (kj/mol)
AlLi	-20	CPD	[6]	
	-20.68	CPD	[24]	
	-20.7	Al	[25]	-21.399
	-20.4 ± 0.2	DRC	[26]	
	-20.7 ± 0.5	SC	[26]	
Al$_2$Li$_3$	-18.8	CPD	[6]	
	-17.93	CPD	[24]	
	-21	Al	[25]	-18.500
	-19.1 ± 0.4	DRC	[26]	
Al$_4$Li$_9$	-14.9	CPD	[6]	
	-14.25	CPD	[24]	
	-16.8	Al	[25]	-14.530
	-15.1 ± 0.2	DRC	[26]	
AlLi$_2$	14.698	MCSFE	[27]	-15.150

SC : Solution Calorimetric method   CPD : Phase Diagram Calculations
DRC : Direct Reaction Calorimetric method   Al : ab-initio calaculations
MCSFE : Miedema Calculator of Standard Formation Enthalpy

The agreement is very good. Figure 4 Shows the calculated enthalpy of mixing at 973 K, 879 K and 1023 K in the AL-Li alloy with the experimental determined by [54,55].

The activities of Li at 987 K [56] in the liquid alloy, where the pure liquid Li is chosen as their reference states, is plotted in Figure 5. As first stated by [57], we verified that when the liquid phase is suspended, the

intermetallic compounds are no more stable at high temperatures and disappear at lower temperatures; see Figure 6. At high temperatures, the BCC_A2 terminal solid solution is stable on the Li-rich side, and the FCC_A1 terminal solid solution on the AL-rich side, between these single-phase domains the two-phase domain (BCC_A2 + FCC_A1) is well calculated.
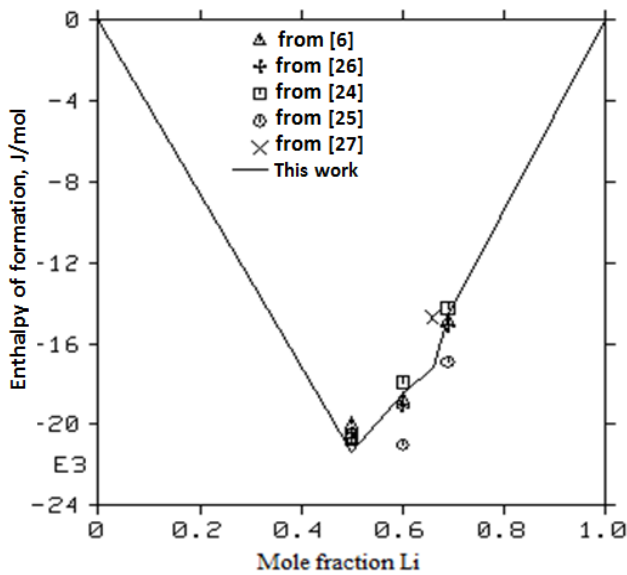

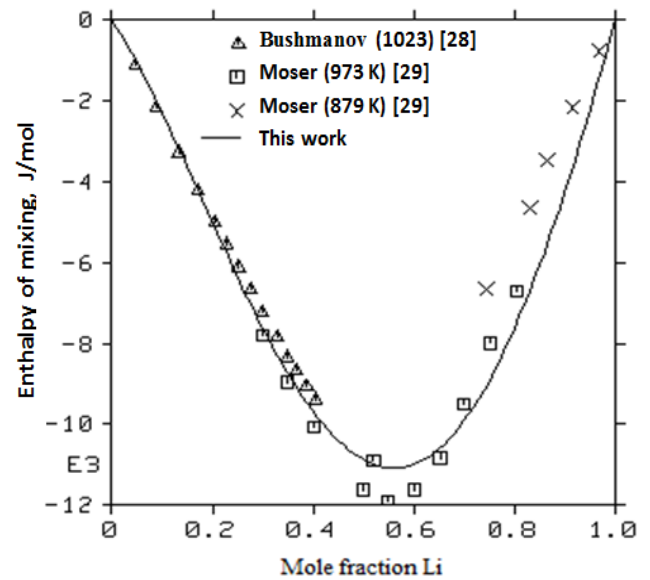**Figure 3:** Calculated and measured enthalpies of formation of the intermetallic compounds.

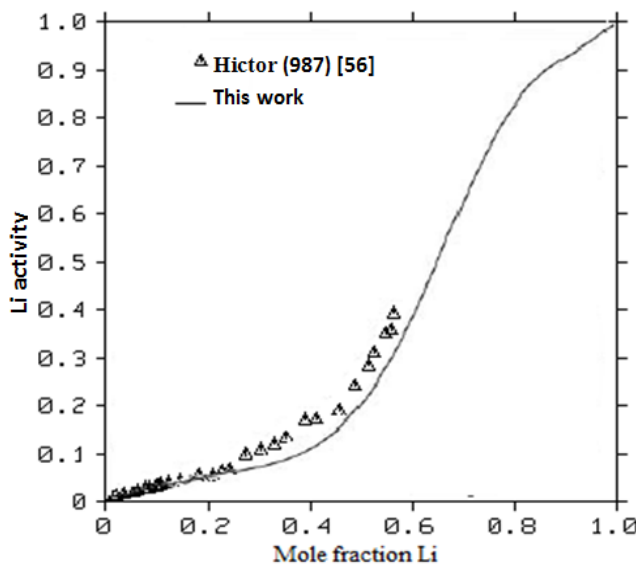**Figure 4:** Calculated enthalpy of mixing in the liquid phase including experimental data [28, 29].

Figure 5: Calculated activity of Li in liquid Al-Li alloys at 987 K compared with experimental data [56].
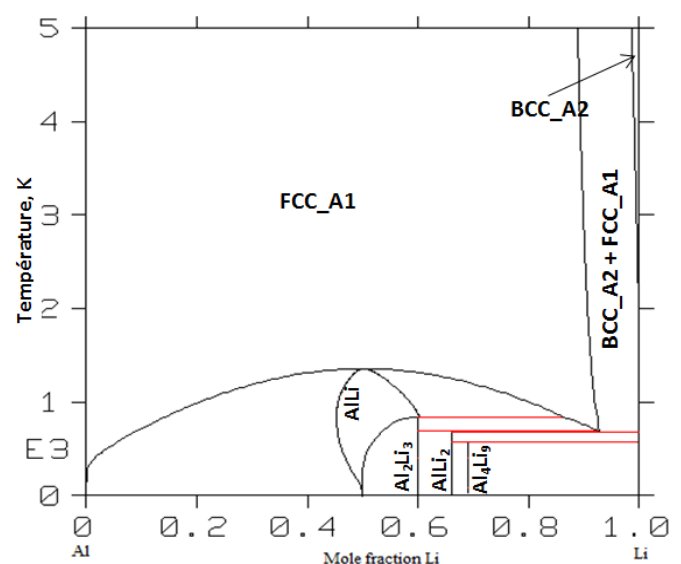

Figure 6: Al-Li calculated phase diagram when the liquid phase is suspended.

Finally, we verified that no miscibility gap was calculated with our thermodynamic optimized parameters as commended in [58]. Figure 7 shows the evolutions of Gibbs energy for the liquid phase as a function of temperature (T), when T is increasing up to 5000 K, the Gibbs energy for the liquid phase decreases. No anomaly is detected on all the curves.
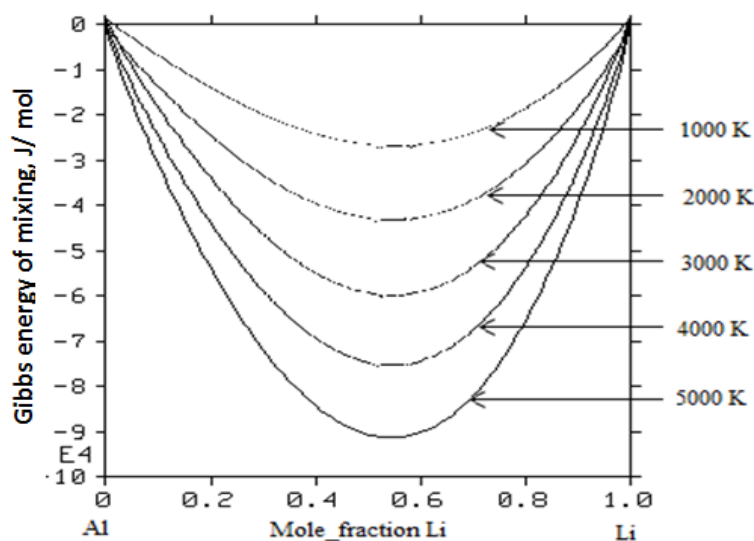
Figure 7: Gibbs energy of mixing of the liquid phase at different temperature.
The reference states were Al and Li liquids.

Conclusion

The present work reviewed critically the experimental information on phase diagram and a thermodynamic property of the Al-Li binary system has been optimized using the CALPHAD method. A set of self-consistent thermodynamic parameters formulating the Gibbs energies of various phases in the Al-Li binary system was obtained, which can reproduce well most of the experimental data on thermodynamic properties and phase diagram. In conclusion, the present optimization of the thermodynamic parameters of the Al-Li system needed to be carried out, and it led to calculated phase equilibria and thermodynamic properties in good agreement with the numerous experimental results.

References

1. Edgar A., Starke Jr., University of Virginia, Charottesville. USA, 61-97.
2. Salah E., Abdellah M., Kamar E M., El-Etre A Y., J. Mater. Environ. Sci. 6 (3) (2015) 892-901.
3. Kaufman L., Bernstein H., *Computer Calculations of Phase Diagrams.* (1970).
4. Sundman B., Jansson B., Andersson J., *Calphad*. 9 (1985) 153-190.
5. Okamoto H., *J. Phase Equilib. Diff.* 33 (2012) 500-501.
6. Hallstedt B., Kim O., *Int. J. Mat. Res.* 98 (2007) 961- 969.
7. Zatorska G., Pavlyuk V., Davydov V., *J. Alloys Compd.* 333 (2002) 138–142.
8. Puhakainen K., Bostrom M., Groy T., Haussermann U., *J. Solid State Chem.* 183 (2010) 2528- 2533.
9. Lavernia E.J., Grant N.J., J. *Mater. Sci*. 22 (1987) 1521.
10. Flower H.M., Gregson P.J., *Mater. Sci. Technol*. 3 (1987) 81.
11. Gao N., Starink M.J., Davin L., Cerezo A., Wang S.C., Gregson P.J., *Mater. Sci. Technol.* 21 (2005) 1010.
12. Whittingham M.S., *Chem. Rev.* 104 (2004) 4271.
13. Gay E.C., Vissers D.R., Martino F.J., Anderson K.E., *J. Electrochem. Soc*. 123 (1976) 1591.
14. Tebbe K.F., von Schnering H.G., Rüter B., Rabeneck G., *Z.Naturforsch b*. 28 (1973) 600.
15. Hansen D.A., Smith J.F., *Acta Crystallog*. B 24 (1968) 913.
16. Schürmann E., Voss H.J., *Giessereiforschung.* 33 (1981) 33.
17. Pulham R.J., Hubberstey P., Hemptenmacher P., *J. Phase Equilib*. 15 (1994) 587.
18. Levine E.D., Rapperport E.J., *Trans. Metall, Soc*. 227 (1963) 1204.
19. Schürmann E., Geißler I.K., *Giessereiforschung*. 32 (1980) 165.
20. Kishio K., Brittain J.O., *J. Phys. Chem. Solids.* 40 (1979) 933.
21. Wen C.J., Boukamp B.A., Huggins R.A., Weppner W., *J. Electrochem. Soc.* 126 (1979) 2258.

22. Veleckis E., J. Less-Common Met. 73 (1980) 49.
23. Amezawa K., Yamamoto N., Tomii Y., Ito Y., *J. Electrochem.* Soc. 146 (1999) 1069.
24. Saunders N., *Z. Metallkde.* 80 (1989) 894- 903.
25. Sluiter M., Watanabe Y., Kawazoe Y., *Phys. Rev.* 53 (1996) 6137-6151.
26. Gasior W., Debski A., Goral A., Major R., *J. Alloys Compd.* 586 (2014) 703-708.
27. De Boer F.R., Boom R., Mattens W.C.M., Miedema A.R., Niessen A.K., North-Holland, Amsterdam. 1988.
28. Bushmanov V.D., Yatsenko S.P., *J. Phys. Chem.* 55 (1981) 1680.
29. Moser Z., Sommer F., Predel B., *Z. Metallkd.* 79 (1988) 705.
30. Lee J.J., Sommer F., *Z. Metallkd.* 76 (1985) 750.
31. Hicter J.M., Vermandé A., Ansara I., Desré P., *Rev. int. hautes Tempér. Réfract.* 8 (1971) 197.
32. Yatsenko S.P., Saltykova E.A., *J. Phys. Chem.* 48 (1974)1402.
33. Aßmann P., *Z. Metallkd.* 18 (1926) 51.
34. Müller A., *Z. Metallkd.* 18 (1926) 231.
35. Grube G., Mohr L., Breuning W., *Z. Elektrochem.* 41 (1935) 880.
36. Shamray F.I., Saldau P.Y., *Izv. Akad. Nauk SSSR.* (1937) 631.
37. Jansson B., Thesis, Royal Institute of Technology, Stockholm Sweden. 1984.
38. Redlich O., Kister A*., Ind. Eng. Chem.* 40 (1948) 345-348.
39. Saunders N., *Z. Metallkd.* 80 (1989) 894.
40. Hillert M., Staffansson L.I., *Acta. Chem. Scand.* 24 (1970) 3618.
41. Dinsdale A.T., *Calphad,* 15 (1991) 317-425.
42. Gue C., Liang Y.L., Li C., Du Z., *Calphad.* 35 (2011) 54–65.
43. Wagner C., Schottky W., *Z. Phys. Chem.* B11 (1930) 163-210.
44. Müller A., *Z. Metallkd.* 18 (1926) 231.
45. Amezawa K., Yamamoto N., Tomii Y., Ito Y., *J. Electrochem. Soc.* 146 (1999) 1069-1074.
46. Cocco G., Fagherazzi G., Schiffini L., *J. Appl. Crystallogr,* 10 (1977) 325-327.
47. Kishio K., Brittain J.O., *J. Phys. Chem. Solids,* 40 (1979) 933-940.
48. Williams D.B., Edington J.W., *Met. Sci,* 9 (1975) 529-532.
49. Shamray F.I., Saldau P.Y., *Izv. Akad. Nauk SSSR.* (1937) 631.
50. Myles K. M., Mrazek F. C., Smaga J. A., Settle J. L., *Argonne National Laboratory.* B50 (1976) 76-78.
51. Pulham R.J., Hubberstey P., Hemptenmacher P., *J. Phase Equilib.* 15 (1994) 587-590.
52. Wen C.J., Boukamp B.A., Huggins R.A., Weppner W., *J. Electrochem. Soc.* 126 (1979) 2258-2266.
53. Schürmann E., Voss H. J., *Alloys Giessereiforschung.* 33 (1981) 43-46.
54. Bushmanov V.D., Yatsenko S.P., *J. Phys. Chem.* 55 (1981) 1680-1681.
55. Moser Z., Sommer F., Predel B., *Z. Metallkd.* 79 (1988) 705.
56. Hicter J.M., Vermandé A., Ansara I., Desré P., *Rev. int. hautes Tempér. Réfract.* 8 (1971) 197-200.
57. Chen S.L., Daniel S., Zhang F., Chang Y.A., Oates W.A., Schmid-Fetzer R., *J. Phase Equilib.* 22 (2001) 373-378.
58. Kaptay G., *Calphad.* 28 (2004) 115-124.